A CFD code comparison of wind turbine wakes

Laan, van der, Paul Maarten; Storey, R. C.; Sørensen, Niels N.; Norris, S.E.; Cater, J. E.

Published in:
Journal of Physics: Conference Series (Online)

Link to article, DOI:
10.1088/1742-6596/524/1/012140

Publication date:
2014

Document Version
Publisher's PDF, also known as Version of record

A CFD code comparison of wind turbine wakes

2014 J. Phys.: Conf. Ser. 524 012140

(http://iopscience.iop.org/1742-6596/524/1/012140)

A CFD code comparison of wind turbine wakes

M. P. van der Laan[1], R. C. Storey[2], N. N. Sørensen[1], S. E. Norris[3], J. E. Cater[2]

[1]Technical University of Denmark, DTU Wind Energy, Risø Campus, Frederiksborgvej 399, 4000 Roskilde, Denmark
[2]The University of Auckland, Department of Engineering Science, 70 Symonds St, Grafton, Auckland 1010, New Zealand
[3]The University of Auckland, Department of Mechanical Engineering, 20 Symonds St, Grafton, Auckland 1010, New Zealand

E-mail: plaa@dtu.dk

Abstract. A comparison is made between the EllipSys3D and SnS CFD codes. Both codes are used to perform Large-Eddy Simulations (LES) of single wind turbine wakes, using the actuator disk method. The comparison shows that both LES models predict similar velocity deficits and stream-wise Reynolds-stresses for four test cases. A grid resolution study, performed in EllipSys3D and SnS, shows that a minimal uniform cell spacing of 1/30 of the rotor diameter is necessary to resolve the wind turbine wake. In addition, the LES-predicted velocity deficits are also compared with Reynolds-Averaged Navier Stokes simulations using EllipSys3D for a test case that is based on field measurements. In these simulations, two eddy viscosity turbulence models are employed: the k-ε model and the k-ε-f_P model. Where the k-ε model fails to predict the velocity deficit, the results of the k-ε-f_P model show good agreement with both LES models and measurements.

1. Introduction

Over the last few decades, wind turbine wakes have become an important research topic in wind energy, because wake turbulence can increase loading on wind turbines and cause power loses in wind farms [1]. Simulating wind turbine wakes in Computational Fluid Dynamics (CFD) is one way of providing a better understanding of the flow around a wind turbine and the wake interaction in a wind farm. Large-Eddy Simulation (LES) is one possible CFD method, but it is relatively expensive to solve for a wind turbine wake [2]. Alternatively, Reynolds-Averaged Navier-Stokes (RANS) methods are relatively cheap, but RANS methods need a high level of turbulence modeling, which has been shown to dominate the flow solution completely [3, 4, 2]. The widespread k-ε Eddy-Viscosity Model (EVM) is known for under-predicting the velocity wake deficit, which is related to the fact that the eddy-viscosity coefficient C_μ is a constant in the k-ε EVM. In previous work, a simple modification to the k-ε EVM was made that solves this problem [2]. In the modified k-ε EVM, known as the k-ε-f_P EVM, a variable C_μ is used, that is a scalar function of the local shear. In regions with high shear, e.g. the edge of a wind turbine wake, C_μ is much lower compared to the original k-ε EVM. As a result, the eddy-viscosity in the wind turbine wake decreases and the recovery of the velocity deficit is delayed. The k-ε-f_P EVM is developed in EllipSys3D, a CFD code developed at the Technical University of Denmark [5, 6]. The calibration of k-ε-f_P EVM is performed with the LES model from

EllipSys3D. In the current work, the results of the k-ε-f_P EVM and the results of the LES model from EllipSys3D are compared with SnS, a LES model developed at the University of Sydney and the University of Auckland [7]. The main goals of the paper can be summarized as:

- A comparison of the LES model of EllipSys3D with the LES model of SnS.
- A validation of the k-ε-f_P EVM with the LES model of SnS.

The paper is focused on comparing the LES model of EllipSys3D with the one of SnS, for four test cases, ranging from a wind turbine in uniform, laminar flow to a wind turbine in a turbulent atmospheric boundary layer (ABL). The results can be used to establish a good practice for wake simulations using LES. In the last test case, the results of the LES models are compared with those of the k-ε EVM, k-ε-f_P EVM and measurements. The test cases and simulations methods are described in section 2. The results of the simulations are presented and discussed in section 3.

2. Methodology

2.1. EllipSys3D

EllipSys3D is a curvilinear, implicit, non-staggered, finite volume code, which can perform RANS simulations and Detached-Eddy Simulations (DES). The SIMPLE algorithm [8] is used to solve the Navier-Stokes equation and the convective terms are discretized with the QUICK scheme [9]. The pressure equation is solved with a Rhie-Chow algorithm that is adapted to model body forces correctly [10, 11]. The DES model of the EllipSys3D code operates as a RANS model close to walls, where all/most turbulent length scales are smaller than what can be resolved by the actual cell size. Away from walls, where the computational cells are capable of resolving the large scales of the turbulence the model reduces to a Smagorinsky model and operates in LES mode. As the present domain does not have any walls, the wall being modeled as a symmetry boundary, the model operates in its LES mode in the full domain. For the remaining part of the paper, the turbulence model is simply referred to as LES.

2.2. SnS

SnS is a Cartesian, fractional step, non-staggered, finite volume, LES code. The convective terms are normally treated with a central difference scheme, however, in the present work the QUICK scheme [9] is employed to promote a fair comparison with EllipSys3D. Note that the difference between the central difference scheme and the QUICK scheme is small, as long as inflow turbulence is present, as shown in section 3.3. The time integration of the convective terms is carried out with an Adams-Bashforth scheme. A modified Rhie-Chow algorithm [11] is employed to solve the pressure equation including body forces, which is similar to one in EllipSys3D, but independently developed. SnS uses a Smagorinsky sub-grid scale model [12] to account for the unresolved turbulence scales.

2.3. Test cases

In table 1, four test cases are listed that are used to compare EllipSys3D with SnS. The test cases are ranked by complexity, starting with the simplest. The first three test cases are based on a NREL-5MW wind turbine [13] in a uniform mean flow, in which walls are absent. This wind turbine has a rotor diameter D and a hub height z_H of 126 m and 90 m, respectively. The last test case is based on field measurements of the Nibe B wind turbine with $D = 40$ m and $z_H = 45$ m. In this test case an ABL is modeled, by placing a wall at the bottom of the domain. In all NREL-5MW cases a free-stream velocity at hub height $U_{H,\infty}$ of 8 m/s is used. The Nibe case is simulated with $U_{H,\infty} = 8.5$ m/s and a turbulence intensity at hub height $I_{H,\infty} \equiv \sqrt{2/3k}/U_{H,\infty}$ of 8% (note that k is the turbulent kinetic energy).

Test case one is a wind turbine in a steady laminar flow and it is designed to compare the wind turbine modeling of EllipSys3D with the one in SnS, without the influence of the turbulence

models. The Reynolds number $Re_D = U_{H,\infty}D/\nu$ is based on the free-stream velocity at hub height $U_{H,\infty}$ m/s, the rotor diameter D m and the molecular kinematic viscosity ν. Re_D is set to 1000 by lowering ν close to unity. The second test case has a high Re_D, in which a standard value for ν is used ($\nu = 1.46 \times 10^{-5}$). Hence, the LES turbulence models are used and the resulting wake flow can be compared. The third test case is the same as second test case, however, isotropic inflow turbulence is added to the simulation. Test case four is a simulation of a wind turbine in a turbulent ABL and it is also simulated with the k-ε EVM and the k-ε-f_P EVM from EllipSys3D.

Table 1. Summary of cases and corresponding input parameters for numerical computations.

Case	Description	Re_D	$I_{H,\infty}$
1	NREL-5MW in a steady laminar uniform flow.	1000	-
2	NREL-5MW in a turbulent uniform flow, without inflow turbulence.	7×10^7	-
3	NREL-5MW in a turbulent uniform flow, with inflow turbulence.	7×10^7	7.8%
4	Nibe B in a turbulent ABL.	2×10^7	8.0%

2.4. General setup

The flow domains of the four test cases from table 1 are illustrated in figure 1, in which the flow domain of the first three test cases is shown. The dimensions of all flow domains are $25\text{D} \times 16\text{D} \times 16\text{D}$. Inside the flow domain, a wake domain is defined of dimensions $13\text{D} \times 2\text{D} \times 2\text{D}$, which starts at $x = 0$. In the uniform flow test cases (cases one to three), the wake domain is placed in the center of flow domain in the y and z-direction, as shown in figure 1. The wake domain in the ABL case is placed at the bottom of the flow domain at $z = 0$, while keeping the central location in the y-direction. The wake domain is discretized by an uniform spacing of D/30 in all three directions. Outside the wake domain, the cells are stretched towards the boundaries with a maximum expansion ratio of 1.2. EllipSys3D and SnS use an identical grid.

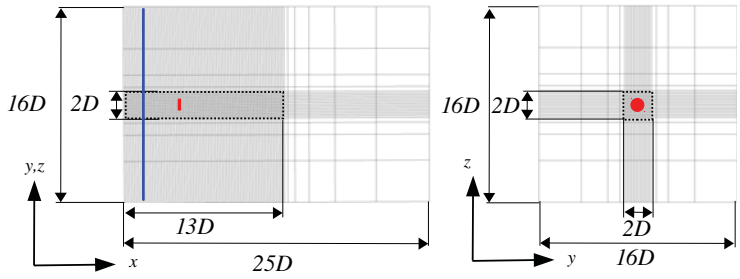

Figure 1. Computational domain for the uniform flow test cases. Left: side/top view. Right: front view. Dashed box marks the wake domain. AD is illustrated as a red box. Blue line represents the inflow turbulence plane. One in every four nodes is shown.

In the uniform flow test cases the side walls at $y = 0$, $y = L_y$, $z = 0$ and $z = L_z$ are periodic boundaries. A uniform mean velocity of $U = 8$ m/s is set at the inlet, located at $x = 0$. The end of domain, at $x = L_x$, is an outlet at which a fully developed flow is assumed. In the ABL test case the bottom wall at $z = 0$ is a slip wall. The side boundaries at $y = 0$ and $y = L_y$ are periodic boundaries. A stream-wise velocity profile U is set at the inlet at $x = 0$ and $z = L_z$.

The profile is set to a (neutral) log law profile for $z > 1/20 z_H$:

$$z > \frac{1}{20} z_H : \; U(z) = \frac{u_*}{\kappa} \ln\left(\frac{z}{z_0}\right), \qquad z \leq \frac{1}{20} z_H : \; U = U\left(\frac{1}{20} z_H\right) \tag{1}$$

where z is the wall normal direction, z_H is the hub height of the Nibe B wind turbine, u_* is the friction velocity, z_0 is the roughness height and $\kappa = 0.4$ the Von Karman constant. The velocity is kept constant for $z \leq 1/20 z_H$ to comply with the slip wall condition. The roughness height is set to 0.07 m and the friction velocity is set such that the velocity at hub height is 8.5 m/s. The end of the flow domain, at $x = L_x$, is set to be an outlet.

In the cases where inflow turbulence is present (cases three and four), a plane is defined on which velocity fluctuations are injected into the flow domain. The location of the turbulence plane is illustrated as a blue line in figure 1. The turbulence plane has the size of the cross section of the flow domain. In SnS the turbulence can only be injected at the inlet. In EllipSys3D the turbulence plane cannot be set directly at the inlet because the velocity fluctuations are inserted as body forces, which are smeared out with a Gaussian filter (using a smearing parameter equal to three cells). Therefore, the turbulence plane is located at 1D downstream from the inlet. In order to keep the distance from the turbulence plane to the wind turbine constant, the wind turbine is placed at 4D and 5D from the inlet in SnS and EllipSys3D, respectively. The generation of the inflow turbulence is discussed further in section 2.6.

2.5. Wind turbine modeling

The wind turbine is modeled as an Actuator Disk (AD) [14, 3]. The AD represents the geometry of the rotor as a disk of size D, on which the blade forces are distributed over the radius and spread out uniformly over the annulus. The AD forces are added as a sink in the momentum equations. In the NREL-5MW cases, a calculated blade force distribution $q(r)$ of the NREL-5MW [15], using a DES of the full rotor geometry, is used as a reference. The result is plotted in figure 2. For simplicity, only the thrust force (thrust coeffient is 0.79) is used and the AD forces are kept constant over time. In the Nibe case, the force distributions are pre-calculated with an actuator line simulation [16] using airfoil data of the Nibe wind turbine [17]. Both the thrust and the tangential force distribution (with thrust and power coefficients of 0.89 and 0.46, respectively) is used such that a comparison with the measurement can be made.

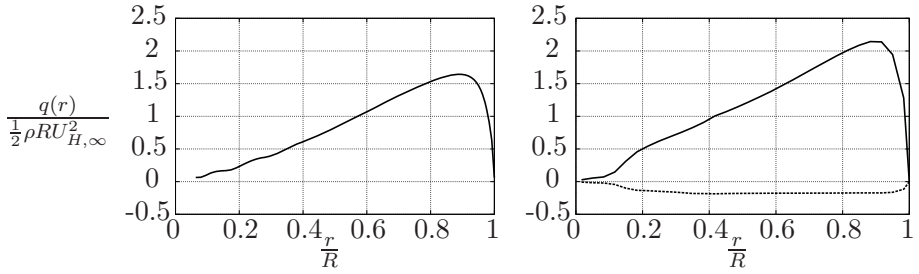

Figure 2. Calculated force distributions $q(r)$. Left: NREL-5MW thrust force. Right: Nibe thrust force (solid line) and tangential force (dashed line).

In SnS the AD forces are generally smeared to neighboring cells using a 1D Gaussian filter. In the current work the force smearing is switched off because EllipSys3D does not use a Gaussian filter to distribute the forces.

2.6. Inflow turbulence

Synthetic inflow turbulence is injected in test cases three and four of table 1. The inflow turbulence is modeled with the Mann model [18]. In an ideal code comparison, the same inflow

perturbations should be used for both LES models, because different turbulence fields can result into different wake solutions. However, this is not possible for the present research due to different implementations of inserting the turbulent fluctuations from the Mann model into the flow domain. It is therefore chosen to generate the Mann turbulence in SnS and EllipSys3D, individually, using the same Mann model parameters. The Mann turbulence is generated in a domain with a cross dimension of the size 16D×16D, using 128×128 cells, with a uniform spacing of D/8. The length of the domain is set long enough to simulate one hour of transient data, including spin-up time. In case three, isotropic turbulence is generated by setting Γ to zero. The length scale L is set to 29.4 m, which is a recommended value from the IEC standard [19] for large wind turbines. The $\alpha\epsilon^{2/3}$ parameter is tuned to get a turbulence intensity of 10% at the turbulence plane, which results in a turbulence intensity of 7.8% at the wind turbine location. In both EllipSys3D and SnS, using $\alpha\epsilon^{2/3} = 0.3$ is sufficient. The (anisotropic) ABL turbulence in case four (Nibe B) is generated with a roughness height of 0.07 m, a hub height of 45 m, a hub height velocity of 8.5 m/s and $\Gamma = 3.9$. The resulting turbulence intensity at the location of the wind turbine at hub height is 8.0% in both LES models.

2.7. RANS setup

Test case four from table 1 is used to compare the LES with two RANS simulations. The setup of the RANS simulations and applied turbulence models is discussed in detail in the work of van der Laan et al. [2] and is briefly discussed here. The flow domain is similar to the one used in the LES, however, only a uniform cell spacing of D/10 is applied in the wake domain, which is based on a grid study that is performed in previous work [2, 15]. The boundary conditions are same as used in LES, however, a rough wall is used instead of a slip wall, where the wall stress and the turbulent dissipation ε are specified at the first cell. A Neumann condition is applied for the turbulent kinetic energy k. The analytical log law solution for U, k and ε is specified at the inlet. The turbulence intensity is set by changing the roughness height z_0, while leaving C_μ equal to 0.03. Subsequently, the friction velocity u_* is adapted to retain the desired hub height velocity of 8.5 m/s. This method results in a slightly modified log law solution, however, the difference in stream-wise velocity in the swept area is smaller than 3% for test case four.

3. Results and Discussion

The results of each test case from table 1 are presented and discussed individually, in the four proceeding sections. The standard deviations taken over the six bins are plotted as error bars. The Nibe case (case four) the LES results are computed with sixty one-minute bins to comply with the post processing of the measurements.

3.1. Test case one: NREL-5MW in a steady laminar uniform flow

The first test case is the NREL-5MW wind turbine in a steady laminar uniform flow. Since a turbulence model is redundant, the test case is ideal to investigate the forcing of the AD applied in EllipSys3D and SnS. In figure 3, the velocity deficit at hub height is plotted for the cross-coordinate y, for three stream-wise distances: at 0D, 2.5D and 7.5D downstream of the AD. The velocity deficit at the AD should be a footprint of the applied forces at the AD.
Even though the same thrust force distribution of figure 2 is used in EllipSys3D and SnS, the resulting velocity deficit at the AD is slightly different at the center of the AD. This difference remains further downstream. The cause of the difference in velocity deficit is not completely understood, however, a plausible reason could be related to the different implementations of the modified Rhie Chow algorithm, that treats the AD forces as pressure jumps at the cell faces. Overall, very good agreement is achieved.

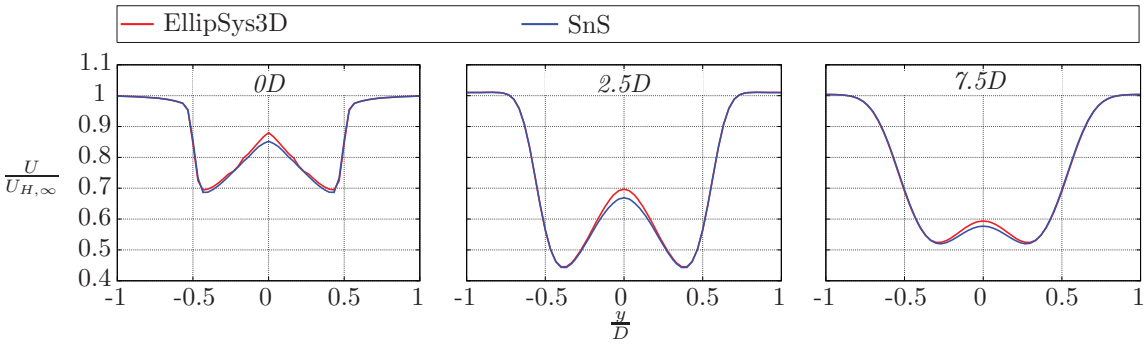

Figure 3. Test case one: NREL-5MW in a steady laminar uniform flow. Velocity deficit at hub height.

3.2. Test case two: NREL-5MW in a turbulent uniform flow, without inflow turbulence
The velocity deficit at hub height, at 0D, 2.5D and 7D, are shown in figure 4, for a the NREL-5MW wind turbine in a turbulent uniform flow. Two results of SnS are shown that are computed with the QUICK scheme and the central difference scheme. The velocity deficit at 7.5D shows that the wake breaks up when the central difference scheme is used. On the contrary, the velocity deficit computed with the QUICK remains stable at 7.5D. The QUICK scheme adds numerical diffusion that stabilizes the wake, while the central difference scheme produces an instable wake at 7.5D. Comparing EllipSys3D and SnS using QUICK, there is a difference in the velocity deficit at 0D, that remains visible further downstream, as discussed in the laminar test cast of section 3.1. In addition, the edge of the wake deficit at 2.5D is sharper in EllipSys3D, than in SnS, which indicates that SnS is more diffusive.

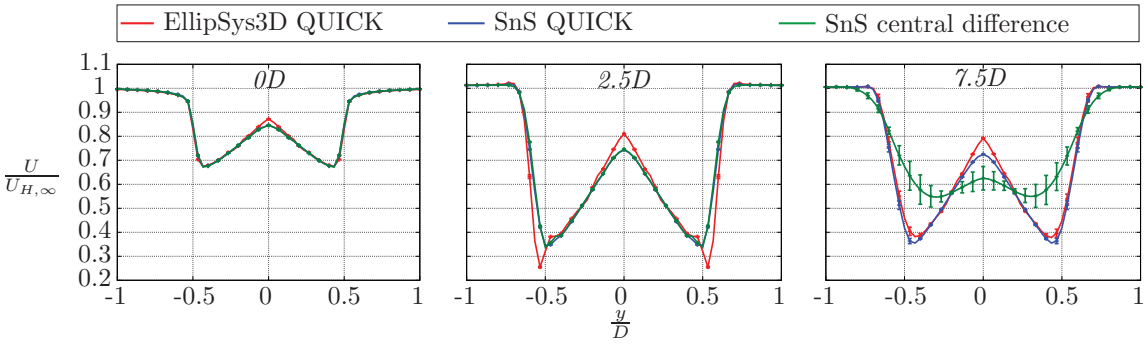

Figure 4. Test case two: NREL-5MW in a turbulent uniform flow, without inflow turbulence. Velocity deficit at hub height.

3.3. Test case three: NREL-5MW in a turbulent uniform flow, with isotropic inflow turbulence
The results of the third test case are presented in figures 5, 6 and 7. In figure 5, a comparison of EllipSys3D and SnS is made for a grid size that corresponds to a uniformly discretized wake domain with a cell spacing of D/30. The influence of the cell spacing in the wake domain is investigated in EllipSys3D and SnS, in figures 6 and 7, respectively. Note that only every second standard deviation is shown in the results of the two finest grid levels.

The velocity deficit and the stream-wise Reynolds-stress are plotted in figure 5, at downstream distances 0D, 2.5D and 7.5D. Two results of SnS are shown that correspond to the QUICK and the central difference scheme. The influence of the numerical scheme is on the velocity deficit and Reynolds-stresses is small. On the contrary, a large difference between the results of the

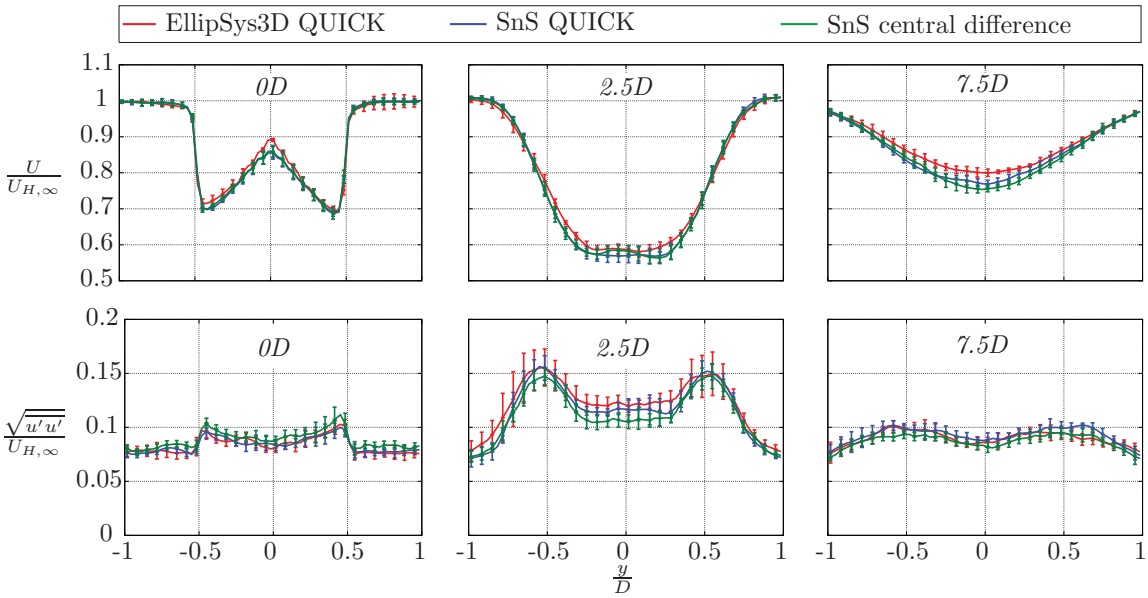

Figure 5. Test case three: NREL-5MW in a turbulent uniform flow, with isotropic inflow turbulence. Velocity deficit (top) and stream-wise Reynolds-stress (bottom) at hub height.

QUICK and the central difference scheme is observed in the turbulent test case without inflow turbulence of section 3.2. Hence, when inflow turbulence is present in the simulation, the choice between the QUICK and the central difference scheme is not important.

Comparing EllipSys3D with SnS using the QUICK scheme, there is a small difference in the velocity deficit at 2.5D, which is more pronounced at 7.5D. It is believed that the difference in generated turbulence field, that is used in EllipSys3D and SnS, is the most likely cause for the difference in velocity deficit. Although, the stream-wise Reynolds-stress outside the wake at 0D, shows that the stream-wise intensity of the turbulence fields is similar. In addition, the averaged stream-wise Reynolds-stress at 2.5D and 7.5D calculated by EllipSys3D and SnS, are within each other standard deviations.

Table 2. Domain dimensions and grid sizes.

grid	1	2	3	4
Spacing in wake domain	D/60	D/30	D/15	D/8
Number of cells	3.1×10^7	3.8×10^6	9.2×10^5	5.2×10^5

In the grid resolution study, four different grid size are used, which are characterized by the uniform spacing in the wake domain. The grid sizes are D/60, D/30, D/15 and D/8 and are listed in table 2. Grids one and four correspond to the finest and coarsest grid, respectively. In figure 6 the velocity deficit and the stream-wise Reynolds-stress are plotted at hub height at 0D, 2.5D and 7.5D. The velocity deficit is similar for finest three grids, however, grid four shows deviations with the finer grids at 0D and 2.5D. Surprisingly, all grids predict a similar velocity deficit at 7.5D. The influence of the grid spacing is more visible in the stream-wise Reynolds-stress. Outside the wake, at 0D, the two finest grids predict higher stream-wise turbulence intensities than the two coarsest grids. This indicates that the two coarsest grids cannot resolve the inflow turbulence properly. At 2.5D, only the coarsest grid is under-predicting the stream-wise Reynolds-stress compared to the finer grids, and at 7.5D the difference between all grids is negligible. Hence, if one is only interested in the velocity deficit, a cell spacing of D/15 is

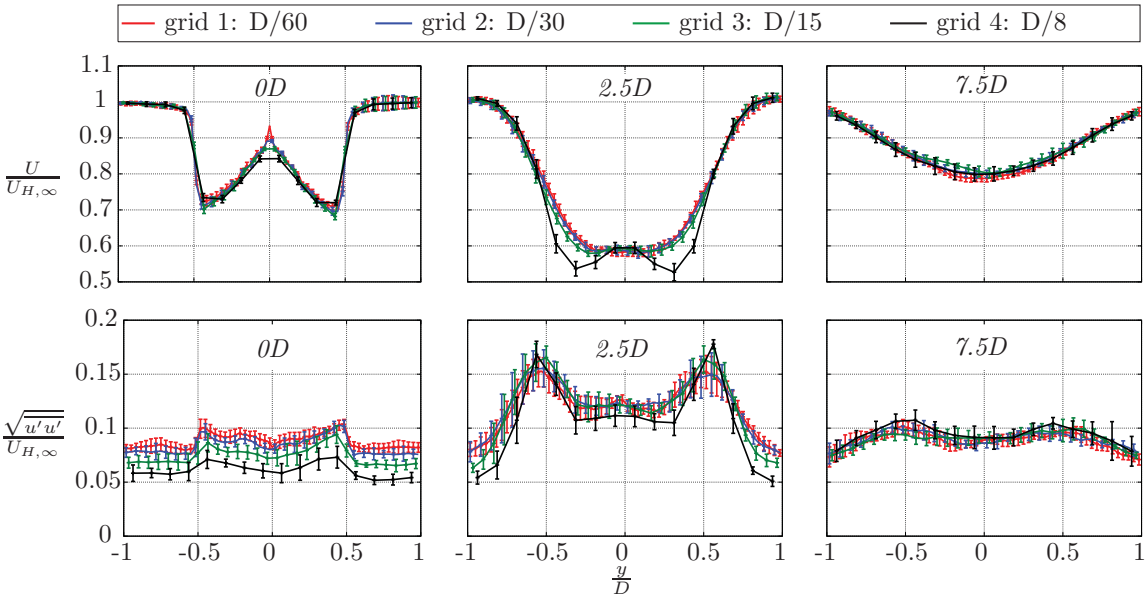

Figure 6. Influence of grid spacing in EllipSys3D for test case three: NREL-5MW in a turbulent uniform flow, with isotropic inflow turbulence. Velocity deficit (top) and stream-wise Reynolds-stress (bottom) at hub height.

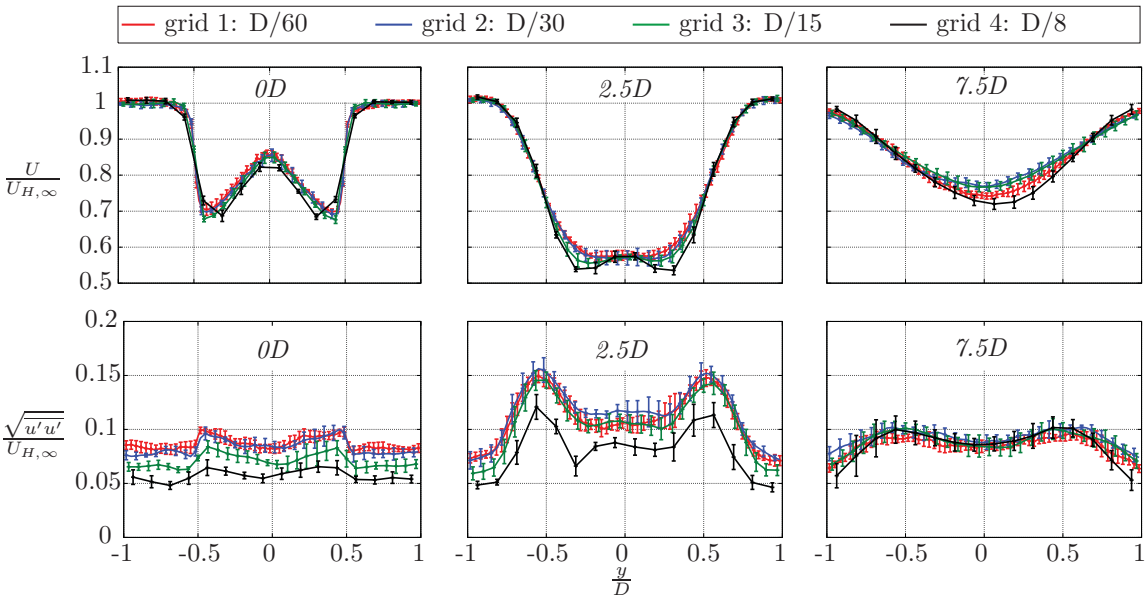

Figure 7. Influence of grid spacing in SnS for test case three: NREL-5MW in a turbulent uniform flow, with isotropic inflow turbulence. Velocity deficit (top) and stream-wise Reynolds-stress (bottom) at hub height.

sufficient enough. However, if the stream-wise Reynolds-stress should be estimated properly, a cell spacing of D/30 is recommended in EllipSys3D.

The grid resolution study in SnS is presented in figure 7, and it shows similar results as the grid study performed in EllipSys3D. However, at 7.5D, the finest grid has a deeper wake deficit compared to the grid two and three, which is not fully understood. In addition, the coarsest grid compares even less well with the finer grids in terms of Reynolds-stresses, as observed in

EllipSys3D. This indicates that a cell spacing of D/8 is not sufficient to resolve a wake in LES. The result of present grid study is in contradiction with the the work of Wu and Porté [20], who showed that their spectral LES model is capable of resolving wakes with a cell spacing of D/7 and D/5 in the wall normal and the cross direction, respectively. While it is known that spectral LES models need less grid points than finite volume methods, the authors find it surprising that a cell spacing of D/5 has been found to be sufficient for spectral LES.

3.4. Test case four: Nibe B in a turbulent ABL

The velocity deficit and the stream-wise Reynolds-stress at hub height as function of relative wind direction are plotted in figure 8. The result of the LES models are also compared with measurements and two RANS simulations using EllipSys3D. One RANS simulation is performed with the standard k-ε EVM, while the other RANS simulation is conducted with a modified k-ε EVM, called the k-ε-f_P EVM [2]. It should be noted that the LES results are computed with sixty one-minute bins to comply with the post processing of the measurements. This increases the standard deviations compared to using six ten-minute bins and it gives an idea of how large the unknown standard deviations of the measurements are.

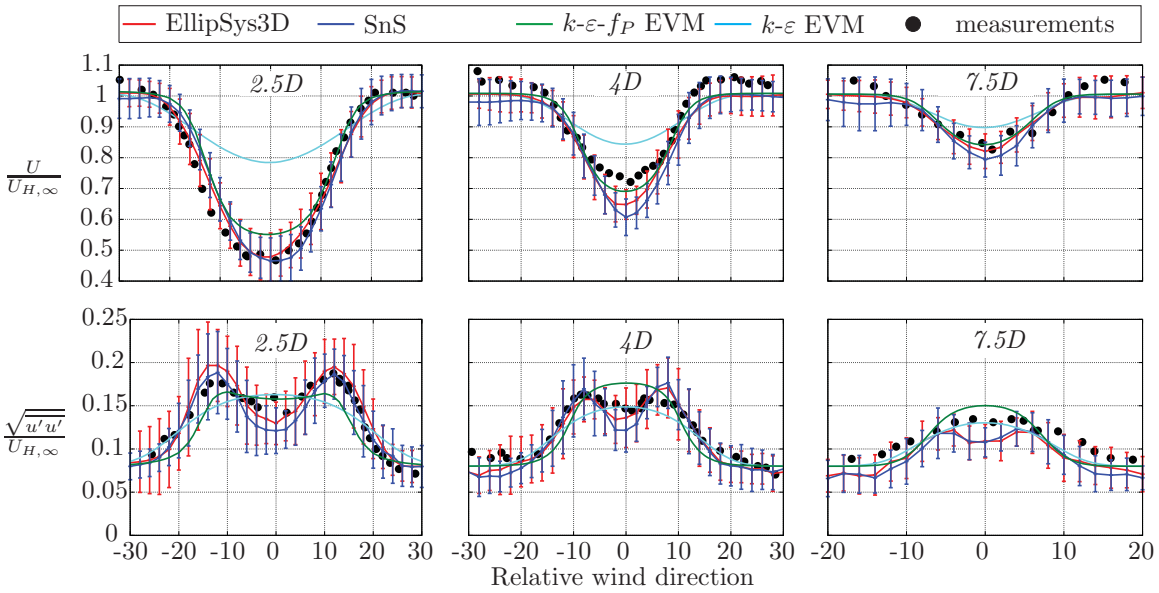

Figure 8. Test case four: Nibe B in a turbulent ABL. Velocity deficit (top) and stream-wise Reynolds-stress (bottom) at hub height.

The results of the LES models compare well each other and with the measurements. Only at 4D the measured velocity deficit is smaller than predicted by of both LES models. However, it is plausible that the measured wake deficit has similar standard deviations as the LES results, which means that the error bars of the measured wake deficit lie within those of the LES models.

The wake deficit calculated by the standard k-ε EVM is underpredicted compared to the measurements and to ones calculated with both LES models, as shown in figure 8. The k-ε-f_P EVM predicts a wake deficit that compares well with both LES models and measurements, at all downstream distances. The variable C_μ that is present in the k-ε-f_P EVM, decreases the eddy-viscosity in the near wake and delays the wake recovery compared to the standard k-ε EVM. Both RANS models show differences in the stream-wise Reynolds-stresses compared to the measurements and LES models. The RANS models can only model isotropic turbulence and are therefore not suited to predict the anisotropic Reynolds-stresses in the wake.

4. Conclusions

The LES model from EllipSys3D is compared with the LES model from SnS using four test cases. The laminar test case shows that the actuator disk implementation is different between the two codes, which results in a small deviation in the velocity deficit. This difference is also observed in the turbulent test case, without turbulent inflow. In the test cases with inflow turbulence, the velocity deficits, the stream-wise Reynolds-stress and the turbulence intensity of the LES models compare well, although there are small differences. It is believed that the use of individually generated turbulence fields, is the main cause of these differences. Overall, a satisfactory agreement is achieved.

The LES mesh study of SnS and EllipSys3D shows that a minimum cell spacing of D/15 is necessary in order to estimate the velocity deficit correctly. However, a cell spacing of at least D/30 is needed if a well resolved stream-wise Reynolds-stress is desired.

The LES models compare well with each other and with the measurements for the Nibe test case. The test case is simulated with the standard k-ε EVM and the k-ε-f_P EVM, employing the RANS model of EllipSys3D. Where the k-ε EVM fails to predict the velocity deficit, the k-ε-f_P EVM shows comparable results with both LES models. Since, the k-ε-f_P EVM is calibrated with the LES model from EllipSys3D, the good agreement of the k-ε-f_P EVM with LES model from EllipSys3D is not a surprise. However, the good comparison of the k-ε-f_P EVM with SnS and measurements validates the k-ε-f_P EVM.

Acknowledgments

This work is supported by the Center for Computational Wind Turbine Aerodynamics and Atmospheric Turbulence funded by the Danish Council for Strategic Research, grant number 09-067216. The authors wish to acknowledge the contribution of the DTU central computing facility and the NeSI high-performance computing facilities at the University of Auckland.

References

[1] Barthelmie R J, Frandsen S T, Nielsen N M, Pryor S C, Réthoré P E and Jørgensen H E 2007 *Wind Energy* **10** 217
[2] van der Laan M P, Sørensen N N, Réthoré P E, Mann J, Kelly M C, Troldborg N, Schepers J G and Machefaux E 2014 *Wind Energy* Pub. online
[3] Réthoré P E 2009 *Wind Turbine Wake in Atmospheric Turbulence* Ph.D. thesis Risø
[4] El Kasmi A and Masson C 2008 *Journal of Wind Engineering and Industrial Aerodynamics* **96** 103
[5] Sørensen N N 1994 *General purpose flow solver applied to flow over hills* Ph.D. thesis DTU
[6] Michelsen J A 1992 Basis3d - a platform for development of multiblock PDE solvers. Tech. rep. DTU
[7] Norris S E, Cater J E, Stol K A and Unsworth C P Dec 2010 *In Proceedings of the 17th Australasian Fluid Mechanics Conference, Auckland, New Zealand*
[8] Patankar S V and Spalding D B 1972 *International Journal of Heat and Mass Transfer* **15** 1787
[9] Leonard B P 1979 *Computer Methods in Applied Mechanics and Engineering* **19** 59
[10] Réthoré P E and Sørensen N N 2012 *Wind Energy* **15** 915
[11] Rhie C M and Chow W L 1983 *AIAA Journal* **21** 1525
[12] Smagorinsky J 1963 *Monthly Weather Review* **91** 99
[13] Jonkman J, Butterfield S, Musial W and Scott G 2009 Definition of a 5-MW Reference Wind Turbine for Offshore System Development Tech. rep. National Renewable Energy Laboratory
[14] Mikkelsen R 2003 *Actuator Disc Methods Applied to Wind Turbines* Ph.D. thesis DTU
[15] Réthoré P E, van der Laan M P, Troldborg N, Zahle F and Sørensen N N 2013 *Wind Energy* Pub. online
[16] Sørensen J N and Shen W Z 2002 *Journal of Fluids Engineering* **124** 393
[17] Taylor G J 1990 Wake measurements on the Nibe turbines in Denmark. National Power Tech. rep. Technology and Environment Centre. ETSU WN 5020
[18] Mann J 1994 *Journal of Fluid Mechanics* **273** 141
[19] International standard IEC 614001, 2005
[20] Wu Y T and Porté Agel F 2012 *energies* **5** 5340